Current Biology 22, 1057–1065, June 19, 2012 ©2012 Elsevier Ltd All rights reserved DOI 10.1016/j.cub.2012.03.066

Article

Genetically Separable Functions of the MEC-17 Tubulin Acetyltransferase Affect Microtubule Organization

Irini Topalidou,[1,4] Charles Keller,[1,4] Nereo Kalebic,[2,4] Ken C.Q. Nguyen,[3] Hannah Somhegyi,[1] Kristin A. Politi,[3] Paul Heppenstall,[2] David H. Hall,[3] and Martin Chalfie[1,*]
[1]Department of Biological Sciences, Columbia University, New York, NY 10027, USA
[2]Mouse Biology Unit, European Molecular Biology Laboratory, Monterotondo 00016, Italy
[3]Albert Einstein College of Medicine, Bronx, NY 10461, USA

Summary

Background: Microtubules (MTs) are formed from the lateral association of 11–16 protofilament chains of tubulin dimers, with most cells containing 13-protofilament (13-p) MTs. How these different MTs are formed is unknown, although the number of protofilaments may depend on the nature of the α- and β-tubulins.
Results: Here we show that the enzymatic activity of the *Caenorhabiditis elegans* α-tubulin acetyltransferase (α-TAT) MEC-17 allows the production of 15-p MTs in the touch receptor neurons (TRNs) MTs. Without MEC-17, MTs with between 11 and 15 protofilaments are seen. Loss of this enzymatic activity also changes the number and organization of the TRN MTs and affects TRN axonal morphology. In contrast, enzymatically inactive MEC-17 is sufficient for touch sensitivity and proper process outgrowth without correcting the MT defects. Thus, in addition to demonstrating that MEC-17 is required for MT structure and organization, our results suggest that the large number of 15-p MTs, normally found in the TRNs, is not essential for mechanosensation.
Conclusion: These experiments reveal a specific role for α-TAT in the formation of MTs and in the production of higher order MTs arrays. In addition, our results indicate that the α-TAT protein has functions that require acetyltransferase activity (such as the determination of protofilament number) and others that do not (presence of internal MT structures).

Introduction

Most microtubules (MTs) are formed from 13 chains, called protofilaments, of α- and β-tubulin dimers [1]. Some cells, however, have MTs with different numbers of protofilaments. Neurons in crayfish and lobster neurons have 12-protofilament (12-p) MTs [2, 3], the sperm of many insects have accessory MTs with 16 protofilaments [4–6], and paramecia [7], cockroach epidermis [8], crayfish sperm [3], and mammalian pillar cells [9] have 15-p MTs. Nematodes are unusual in that none of the cytoplasmic MTs have 13 protofilaments [10, 11]. In *Caenorhabiditis elegans*, the touch receptor neurons (TRNs) have 15-p MTs, whereas all the other cells have 11-p MTs [10].

When cells have a variant MT form, virtually all of the MTs are of that type. In contrast, in vitro polymerization of MT proteins produces MTs that vary in protofilament numbers [12–18]. These observations suggest that components other than the tubulins determine protofilament number and MT fidelity. The protein doublecortin has been suggested to be required for the formation of 13-p MTs [19], but the protein or proteins needed to form variant MTs is not known. We propose that the α-tubulin acetyltransferase MEC-17 and similar proteins play an important role in defining protofilament number.

The *mec-17* gene was originally identified through a touch-insensitive mutant in *C. elegans* [20]. Two groups [21, 22] found that the MEC-17 protein from *C. elegans* and its homologs in other organisms are tubulin acetyltransferases, enzymes that acetylate α-tubulin on the lysine at position 40 [23]. Although *mec-17* is only expressed in the TRNs, *C. elegans* has a second gene that also acetylates α-tubulin, W06B11.1, or *atat-2*, which is expressed in the TRNs and several other cells [21, 22].

mec-17 is exclusively and very highly expressed in the six TRNs [24]. This expression pattern is intriguing, leading to questions of whether MEC-17 may have a unique role in the TRNs, and perplexing, inviting one to wonder why a gene encoding an enzyme should be expressed at such a high level, one even higher than the *mec-12* α-tubulin gene and the *mec-7* β-tubulin genes [24, 25] that are needed for 15-p MTs in the TRNs [20, 26–28].

Another issue arises from the supposed action of tubulin acetyltransferases in the acetylation of lysine 40 in α-tubulin, which is thought to be located on the inner surface of the MT [29]. We were particularly intrigued by this requirement because a striking feature of the 15-p MTs in the TRNs is that they contain material within their lumens [10, 30]. We wondered whether this material could be MEC-17 or a protein dependent on MEC-17 for its localization.

Given these questions, we examined the effect of mutations in *mec-17* and *atat-2* on the structure and organization of MTs in *C. elegans*. We find that production of 15-p MTs in the TRNs requires *mec-17*. Both the number and structure of the MTs are affected. Because the touch insensitivity and some of the TRN morphological defects of the loss of *mec-17* are partially restored using an acetylation-defective version of MEC-17, we suggest that MEC-17 provides both enzymatic and structural functions needed for mechanosensation and TRN axonal morphology. In addition, we find that the luminal material within the TRN MTs requires both MEC-17 and ATAT-2, but MEC-17 can be enzymatically inactive, suggesting that at least MEC-17 may be acting as a structural component. Finally, we present evidence suggesting that MEC-17 may have additional functions independent of 15-p MT formation.

Results

mec-17 and *atat-2* Are Needed for Touch Sensitivity and MEC-12 Acetylation

The original *mec*-17 allele, *u265*, which contains two missense mutations, caused a progressive decrease in touch sensitivity as the animals matured [20, 24]. Subsequently, the *C. elegans* Knockout Consortium [31] produced deletion alleles for both *mec-17(ok2109)* and *atat-2(ok2415)*. With regard to touch sensitivity, we found that *mec-17(ok2109)* animals are considerably touch insensitive and show a slight age-dependent

[4]These authors contributed equally to this work
*Correspondence: mc21@columbia.edu

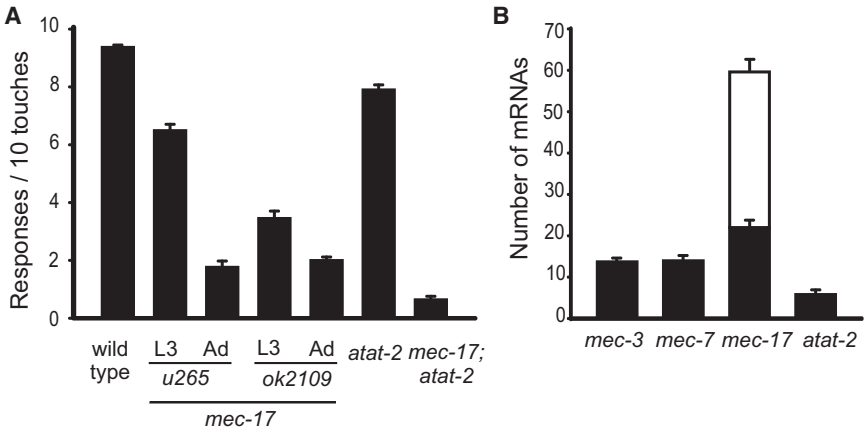

Figure 1. Mutant Phenotype and Expression of *mec-17* and *atat-2*

(A) Touch sensitivity is largely reduced in *mec-17* mutant animals and slightly decreased in *atat-2* mutants (mean ± SEM; n = 30).

(B) PLM neurons in WT larvae have more *mec-17* mRNA (mean number of molecules ± SEM; n = 10) than *atat-2, mec-7* or *mec-3* mRNA. Black bars indicate the number of mRNAs in the cell body and white bars the number of process mRNAs.

See also Figure S1.

increase in touch insensitivity, as compared to animals with the *u265* allele (Figure 1A). Wild-type (WT) animals do not show age-dependent changes in touch sensitivity (not shown). The *atat-2* mutation produces a slight loss of touch sensitivity on its own and a similar decrease in touch sensitivity in combination with *mec-17(ok2109)* (Figure 1A). These results are intermediate between those of Akella et al. [21], who found a dramatic reduction of touch sensitivity in the double mutants, and those of Shida et al. [22], who found no difference in touch sensitivity between the *mec-17* deletion and its double with an *atat-2* deletion. Presumably slight differences in scoring account for this variability.

The need for *mec-17* and *atat-2* in touch sensitivity correlates with their level of expression in the TRNs. *mec-17* is one of the highest expressed genes in the TRNs [24]. We used single molecule fluorescence in situ hybridization (SM-FISH) to show that *mec-17*, in contrast to *atat-2*, is indeed highly expressed in the TRNs; the PLM neurons of WT animals had 60 ± 5 *mec-17* messenger RNA (mRNA) molecules and 6 ± 1 *atat-2* mRNA molecules (Figure 1B). Moreover, *mec-17* mRNA was localized both in the cell body and all along the TRN axon, whereas *atat-2* mRNA was only located in the cell body (see Figure S1A available online). In addition, *mec-17* was expressed solely in the TRNs in contrast to *atat-2*, which was broadly expressed (Figure S1A, see also Shida et al. [22]). Moreover, overexpression of *atat-2* under the *mec-17* promoter in WT animals resulted in touch insensitive animals with morphologically impaired TRNs (seven stable lines and 90% frequency; Figure S1B). (Overexpression of this construct in *mec-17; atat-2* animals did not rescue the touch insensitivity; data not shown.) These defects, which demonstrate a gain-of-function phenotype for *atat-2* overexpression, were never seen when the same amount of *mec-17p::mec-17(+)* was injected into WT or *mec-17; atat-2* mutants. These results argue that MEC-17, in contrast to ATAT-2, has a unique role in the TRNs for which particularly high levels of expression may be needed. Because ATAT-2 cannot replace MEC-17, *mec-17* and *atat-2* are not functionally redundant in the TRNs. *mec*-17 mRNAs could be translated in the TRN processes because the processes do contain ribosomes as can be seen in electron tomograms (see below).

In our hands, deletion of either *mec-17* or *atat-2* alone did not markedly reduce the acetylation of TRN MTs as detected by the antibody 6-11B-1 [32], which recognizes acetylated Lys 40 on α-tubulin. This result agrees with the results of Akella et al. [21] but not with those of Shida et al. [22] who reported a significant decrease in acetylation in both single mutants. This inconsistency could be the result of different immunofluorescence procedures. As previously noted [21, 22], TRNs in *mec-17(ok2109); atat-2(ok2415)* animals have no detectable staining (data not shown).

TRNs in *mec-17* but Not *atat-2* Mutants Exhibit Morphological Defects

In contrast to Shida et al. [22], who reported seeing no gross defects in the TRNs, we found several morphological defects in *mec-17(u265)* and *mec-17(ok2109)* TRNs (Figure 2; Figure S2). ALM and PLM axons in late larvae and young adults were often curved and had apparently swollen regions (Figure 2A; Figure S2A) and infrequent ectopic branches that appeared to derive from the swollen regions (Figure S2A). WT animals and *atat-2* mutants did not show these defects.

Both *mec-17(ok2109)* and *mec-17(u265)* produced an increase in the length of the TRN processes (Figure 2B; Figure S2B). The most dramatic increase was seen in the length of a normally short, or nonexistent, ALM posterior process (Figure 2B). This extraordinary process appeared by 24 hr post hatching (Figure S2C) and was 10 ± 0.9 (mean ± SEM; n = 40) cell body diameters in 1-day-old adults. This posterior ALM process contained acetylated tubulin (data not shown) and showed the characteristic punctate pattern of staining with an antibody against the channel protein MEC-2 (Figure S2D). (Shida et al. [22] report a minor change, 2 μm—about one cell body diameter, in the position of the ALM cell body. We do not see this change (Figure S2E), and such a change would not account for the production of such a long posterior process.) Both the anterior processes of the ALM neurons and the anterior and the posterior processes of the PLM neurons were longer in the *mec-17* mutant strains (Figure 2B; Figure S2B), showing that the effect of *mec-17* on process outgrowth is general.

The TRN morphological defects and touch insensitivity in young *mec-17(ok2109)* adults were caused by the loss of *mec-17*, because WT genomic DNA for *mec-17* rescued all the mutant phenotypes (see below). Deletion of *atat-2* did not produce any of these TRN defects or increase these defects in doubles with *mec-17(ok2109)* (data not shown). In contrast, mutations in the β-tubulin gene *mec-7* fully suppressed all the *mec-17* axonal defects (touch insensitivity, however, could not be tested; data not shown). Because mutation of *mec-7* also causes a *dlk-1*-dependent reduction in TRN protein synthesis [33], the suppression could simply reflect the production of less protein. This hypothesis is unlikely because the same suppression of the *mec-17* defects was seen in *dlk-1; mec-17; mec-7* and *dlk-1; mec-12; mec-17* animals as well as

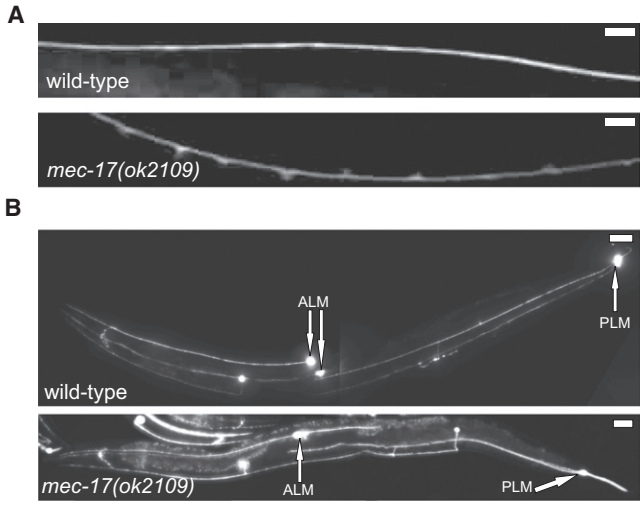

Figure 2. Loss of *mec-17* Alters TRN Morphology

(A) The ALM anterior process of a young *mec-17(ok2109)* adult has many swellings (using *mec-17Δ::gfp*); a similar process in WT does not. Scale bars represent 20 μm.

(B) ALM and PLM processes are longer in a young *mec-17(ok2109)* adult than in a similarly aged wild-type (both express *mec-17Δ::gfp*). The positions of the cell bodies are indicated by arrows. Scale bars represent 100 μm.

See also Figure S2.

dlk-1; mec-17 animals treated with colchicine (Figure S2F; mutation of *mec-7* and *mec-12* or treatment with colchicine does not grossly affect TRN morphology). These results suggest that the *mec-17* morphological defects depend on the *mec-7* and *mec-12* MTs in the TRNs.

Effects on TRN MT Organization and Structure

We used electron microscopy (EM) to determine whether the loss of *mec-17* and *atat-2* affected the TRN MTs. Although the TRN MTs are short compared to the length of the TRN process, the average number of MTs seen in a cross section of the process is fairly constant [30]. Thus, the average number of MTs in a cross-section correlates with the amount of polymerized MTs in the cell. Mutation of either *mec-17* or *atat-2* caused a reduction in the number of MTs per section (Figure 3A). Consistent with their effects on touch sensitivity, MT loss was greater in *mec-17(ok2109)* animals (8.8 ± 0.7, n = 7 cells) than in *mec-17(u265)* animals (14.7 ± 0.8, n = 6), with the former having 5-fold fewer TRN MTs than WT (46.5 ± 0.5, n = 5). The *atat-2* mutation resulted in a small, but consistent, reduction in TRN MTs (31 ± 3.6, n = 7), but not in a statistically significant decrease in MT number in *mec-17(ok2109); atat-2(ok2415)* animals (7.0 ± 0.3, n = 5). MT counts in animals containing *mec-17* mutations may be underestimates because of MT bending (see below). The tilt of bent MTs caused oval cross-sections; in extreme cases, tilting obscured their appearance in standard cross-sections. In other experiments, we viewed sections with multiple tilt angles but could not always find a tilt angle that left all the MTs visible at once.

The *mec-17(ok2109)* and *atat-2* mutations also affected the structure of the TRN MTs (Figure 3; Figure S3). First, the MTs of *mec-17* and *mec-17; atat-2* animals varied in diameter; this variability was not seen in WT and *atat-2* animals (Figure 3A). To understand the basis of this variability, we stained MTs with tannic acid to allow us to count the numbers of protofilaments in electron micrographs. Profound differences were seen in protofilament number with WT and *atat-2(ok2415)* animals containing 15 protofilament MTs (14.9 ± 0.07 and 14.8 ± 0.1, respectively, n = 23), *mec-17(ok2109)*, and *mec-17(ok2109); atat-2(ok2415)* animals containing MTs having from 11–15 protofilaments (13.4 ± 0.2 and 12.7 ± 0.2, n = 23 and 11, respectively) with most (60%) of the MTs having 13-p (Figure 3B).

Second, MTs of a given protofilament number varied in size. Because MTs in some sections were viewed obliquely (and thus appeared as ovals), we used the smallest diameter of the MT profile as a measure of its true diameter. Although the diameters of WT TRN MT are quite uniform, those of the 15-p MTs in *mec-17* and *mec-17; atat-2* mutants were variable (Figure 3B).

Third, mutation in either *mec-17* or *atat-2* affected the appearance of the material within the MTs (Figure 3A). Seventy percent of WT TRN MTs show some sort of material within the MT lumen in electron micrographs (93 of 135 MTs). Often this material is seen as a distinct dot. In contrast, very few of the MTs in other cells (ALN, VCN) have this material. This luminal material was completely missing in *mec-17(ok2109)* animals (45 MTs) and was reduced to approximately 8% in *atat-2(ok2415)* animals (18 of 217 MTs). In the latter case, the luminal material when present was often indistinct. Given that the acetylation of Lys 40 on α-tubulin is found on the luminal surface of the MTs [29], these observations suggest that both MEC-17 and ATAT-2 are necessary for the presence of the luminal material.

Fourth, we found that MTs in *mec-17* TRNs were decorated with apparent tubulin hooks, some of which reattached to form MT doublets and triplets. We noticed several hooks and MT doublets in *mec-17* (two clockwise-curved hooks, two doublets, and one triplet, n = 23 in three animals) and *mec-17; atat-2* (two clockwise-curved hooks, one counter-clockwise-curved hook, two doublets, and one triplet, n = 26 in three animals; Figure 3B). We did not observe any hooks, doublets or triplets in micrographs from WT and *atat-2* mutant animals (n = 44 and 37, respectively, in two animals each).

Mutation of *mec-17* Alters the Organization of TRN MTs

We used electron tomography to compare the 3D structure of ALM MTs in a *mec-17(ok2109)* mutant to those in WT (Figure 4). Within WT ALM processes, MTs formed a single bundle with almost uniform spacing between each MT (Figures 4A–4C, see also [10]). The mutant showed several types of prominent defects, including periodic swellings (presumed to be the "swellings" seen in light micrographs) of the whole ALM process, severe bending of the MTs within the confines of the swelling, and occasional locales where individual microtubules became momentarily indistinct, as if they were partially disassembled over short stretches (Figures 4D and 4E). Most TRN MTs in *mec-17(ok2109)* formed a bundle that ran along the surface of the swellings. A small number of MTs traversed the swelling in an almost straight fashion, whereas many other microtubules that should have also moved as a straight bundle seemed broken and failed to cross the swelling.

These swellings appear to be the consequence of MT bending, because the swellings seen with light microscopy were dynamic structures that changed when the animals moved (see Figure 5; Movie S1). As animals bend, their neurons will be stretched (except for those lying at the midline). For the TRNs, fewer swellings were seen at maximum

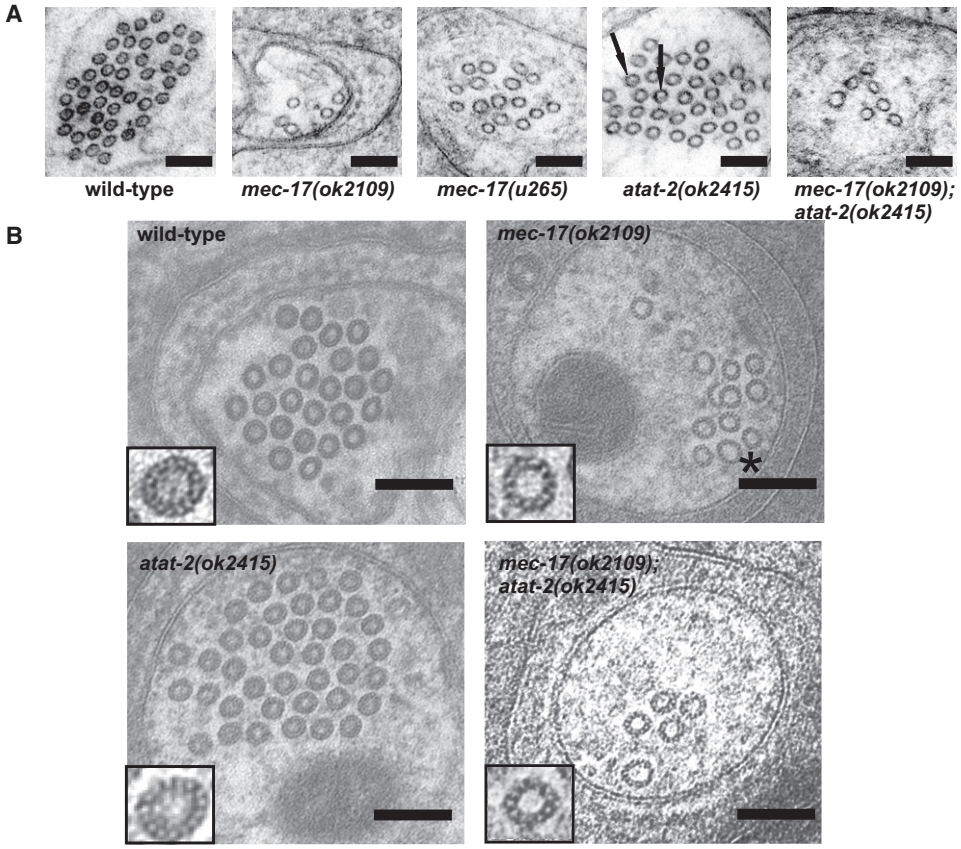

Figure 3. Effects of *mec-17* and *atat-2* Loss on MT and Protofilament Number

(A) Electron micrographs of ALM neurons. Scale bars represent 100 nm. Arrows indicate MTs with luminal material. Animals were fixed in HPF without tannic acid.

(B) MTs have variable numbers of protofilaments in tannic acid-stained *mec-17(ok2109)* and *mec-17(ok2109); atat-2(ok2415)* animals. The asterisk indicates a 15-p MT having larger diameter than the WT 15-p MTs. Note the MT hook in the *mec-17(ok2109)* cell. Scale bars represent 100 nm. Animals were fixed in HPF and tannic acid with the exception of the WT animal that was fixed in glut and tannic acid.

See also Figure S3.

bending of the animals. These results suggest that MTs in the mutants buckled when the cells shortened, causing the production of the swellings and loops.

Enzymatically Inactive MEC-17 Mutants Rescue Some of the *mec-17* Phenotypes

To determine whether the acetyltransferase activity was crucial for MEC-17 function, we tested whether two enzymatically inactive forms of the protein could rescue the various *mec-17* phenotypes. The first catalytically inactive form (dW) was generated by replacing two glycine residues (G121 and G123) with tryptophans in the conserved acetyl coenzyme A (CoA) binding domain, making the protein unable to bind acetyl CoA [34]. The second catalytically inactive form had the MEC-17[D157N] change also studied by Shida et al. [22]. Transformation with either construct in *mec-17; atat-2* mutant animals did not restore Lys 40 acetylation (Figure S4). Both constructs, when expressed in *mec-17* and *mec-17; atat-2* mutant animals, largely rescued the touch insensitivity (Figure 6A) and the production of the posterior ALM process (Figure 6B), but did not prevent the production of swellings and ectopic branches (Figure 6B).

These results contradict those of Shida et al. [22] who reported that the enzymatically inactive MEC-17[D157N] did not rescue the *mec-17* touch defect. Because these authors did not find significant rescue by WT *mec-17* and found a dominant-negative effect with MEC-17[D157N], we feel that their conclusion is not supported by their experiments. One reason for this contradiction may be that we used genomic constructs in our experiments, whereas Shida et al. [22] used complementary DNAs (cDNAs) in Gateway vectors. In preliminary experiments (data not shown), we have not been able to obtain *mec-17* rescue with genomic DNA using the Gateway system.

The number of TRN MTs in *mec-17; mec-17(dW)* and *mec-17; atat-2; mec-17(dW)* mutants were 12 ± 2 (n = 5) and 8 ± 1 (n = 5), respectively (Figure 7). The number of tannic acid-stained protofilaments in MTs in *mec-17; mec-17(dW)* and *mec-17; atat-2; mec-17(dW)* animals was 13.6 ± 0.2 (n = 20) and 12.8 ± 0.2 (n = 20), respectively. These values were equivalent to those found in *mec-17* and *mec-17; atat-2* animals (see above). The luminal material, however, was present in *mec-17; mec-17(dW)* MTs (49 out of 58 MTs, n = 5 animals; Figure 7). In contrast, the luminal material was missing in *mec-17; atat-2; mec-17(dW)* MTs (17 MTs, n = 2).

We conclude that although enzymatically inactive *mec-17* rescued some of the *mec-17* phenotypes, MEC-17-driven acetylation defines the correct protofilament number. Our

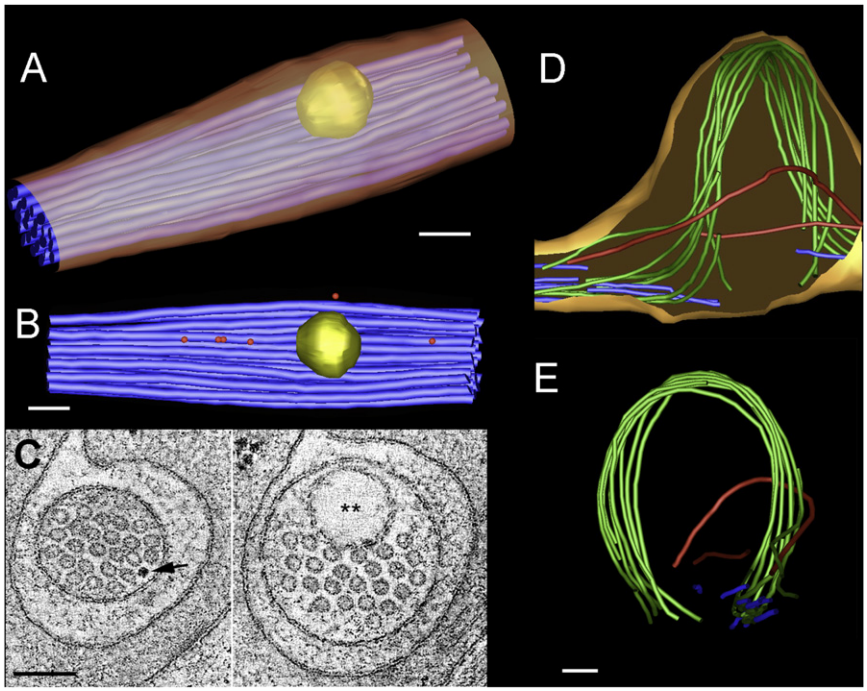

Figure 4. Electron Tomograms of ALM Processes

(A and B) An IMOD model of a WT ALM process is shown from oblique and lateral aspects, respectively, to emphasize the regularity of MTs (blue) within the TRN process. Cargoes lie next to the bundle (ribosomes, red; large vesicle, yellow), and the microtubule bundle deforms locally to admit passage of the vesicle, as does the ALM plasma membrane (gold). Scale bars throughout represent 100 nm.

(C) Two orthoslices through the same WT ALM tomogram are shown. Compare transverse views where the process contains a ribosome (arrow) and a large vesicle (double asterisk).

Other views of the WT ALM tomogram (A–C) have been shown for demonstration purposes on the movie gallery of WormAtlas (http://www.wormatlas.org/movies/pln1_720x480HQ.mov) and in [43], a review of EM methods).

(D and E) Two views of an IMOD model of a large swelling of the mutant ALM process. Three distinct groups of MTs are seen. First, many MTs (blue), which are found outside the swelling, do not pass through it, possibly due to tubule breakage. Second, two other MTs (red) traverse the swelling along independent paths before rejoining the main (blue) bundle on either side. Third, a large bundle of MTs (green) bend dramatically to follow the outer border of the swelling before returning to rejoin the blue bundle on either side. (D) shows the swelling from a lateral aspect. ALM plasma membrane (shown in gold) is closely bound to the limits of the microtubule bundle, as if the membrane has ballooned out to cover the bundle. (E) is a transverse view of the ALM process (compare to similar views of the WT process).

results separate the touch insensitivity and axonal outgrowth defects from the MT structural defects of *mec-17* animals and suggest a non-αTAT role for *mec-17* in the TRNs. In addition, the finding that αTAT activity was not needed for touch sensitivity may explain, at least in part, why only a single EMS-induced allele of *mec-17* has been identified [20].

The rescue by enzymatically inactive MEC-17 and the presence of *mec-17* mRNA in such high amounts and all along the TRN processes prompted us to examine whether *mec-17* mRNA, and not its protein product, rescued touch insensitivity. We transformed *smg-5; mec-17* animals with *mec-17* containing an early stop codon (the *smg* mutation prevents nonsense-mediated decay; [35]), but failed to rescue the *mec-17* phenotypes; the swellings, bends, and extensions remained and the animals were touch insensitive (2.2 ± 0.3 responses out of ten touches, n = 20, four lines). Thus, the function of *mec-17* is protein-dependent. The localization of *mec-17* mRNA and ribosomes along the TRN processes could permit local translation and thus immediate access of the protein to the MTs.

Discussion

The α-tubulin acetyltransferase MEC-17 functions both enzymatically and nonenzymatically to allow mechanosensation, proper axonal morphology, and MT structure. MT number, protofilament number, MT organization, and maintenance of the neuronal process require MEC-17-driven acetylation, but touch sensitivity and the extension of the TRN processes do not. These observations indicate that MEC-17 has an additional function(s) independent of its acetyltransferase activity that is required for touch sensation and process elongation and that the large number of 15-p MTs is not essential for mechanosensation.

Our finding that tubulin acetylation is not necessary for mechanosensation extends the previous findings [21, 28] showing that Lys40 in the MEC-12 is not needed for touch sensitivity. (In contrast, Shida et al. [22] claimed that the partial

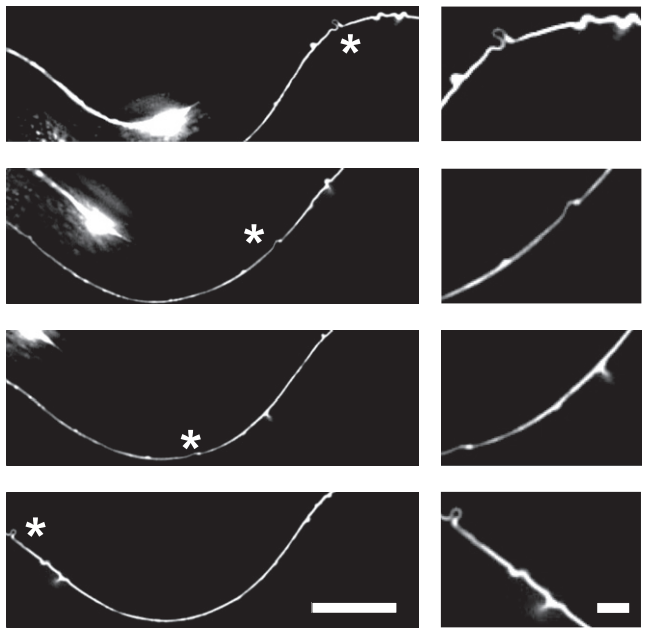

Figure 5. A TRN Axonal Swelling Seen in an L3 stage *mec-17* Mutant Animal Changes as the Animal Moves

Shown are four images from Movie S1. Elimination of the swelling is observed as the axon stretches. Asterisk indicates the position of the swellings. Scale bars represent 5 μm and 1 μm (zoomed image). See also Movie S1.

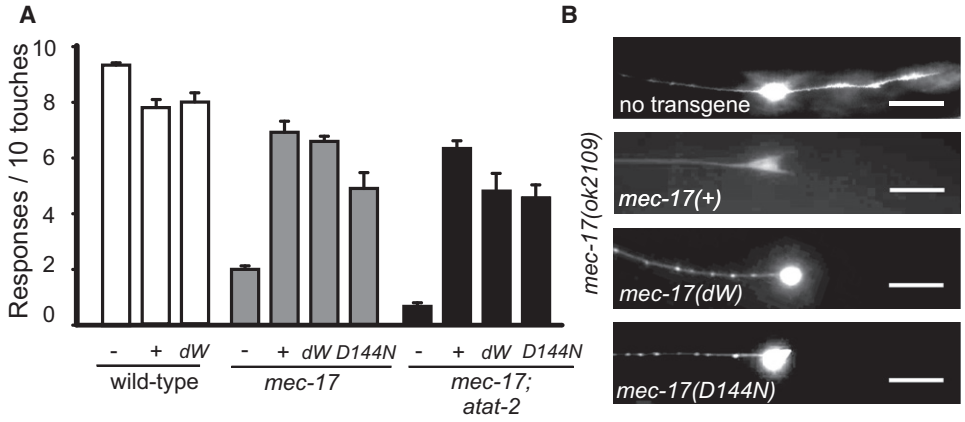

Figure 6. Enzymatically Inactive MEC-17 Rescues Touch Sensitivity and Process Extension in the TRNs

(A) Similar rescue of touch insensitivity occurs with *mec-17(+)* and mutated genes that produce proteins that cannot acetylate MTs (*mec-17dW* and *mec-17D144N*) (n = 20; $p < 0.001$ in all cases) (mean ± SEM).

(B) Enzymatically inactive forms of MEC-17 prevent the production of the posterior ALM process, but not process swelling. Scale bars represent 20 μm. See also Figure S4.

rescue of touch sensitivity of *mec-12; mec-17; atat-2* triple mutants by a MEC-12 mutated to mimic the acetylated protein showed that αTAT-dependent acetylation was needed for touch sensitivity. Because the rescue, however, was only to the level found in *mec-17; atat-2* mutants, their result could be interpreted as a rescue of the absence of *mec-12*.) MEC-17 could play a structural role in touch sensation by functioning as a MT-associated protein (MAP; see also [21]). Interestingly, the α-tubulin deacetylase appears to have a nonenzymatic effect on MT growth in cultured mammalian cells [36].

The number of MTs in the TRNs depends on *mec-17* and, to a lesser extent, *atat-2*, suggesting that acetylation of MEC-12 Lys40 and/or of some other residue or substrate permits the production of the extensive MT bundle. MEC-17 and ATAT-2 could affect initiation of new MT synthesis and/or stabilize the integrity of single microtubules, both of which ought to promote increased numbers and longer MTs. Large, regularly ordered groups of MTs are often seen when the MTs have 15 protofilaments [3, 8, 9]. We suggest that higher expression of an αTAT may be needed for this MT organization.

The loss and/or disruption of luminal staining in electron micrographs in *mec-17* and *atat-2* mutants, and the high expression levels of *mec-17* mRNA in WT cells ([24, 25]; this work), suggest that these two proteins could be needed structurally as well as enzymatically for MT structure and organization, perhaps as MAPs. One appealing function of MEC-17 and ATAT-2 as structural proteins could be in the formation of the luminal materials in the TRN MTs [37], a hypothesis that is supported by our finding that the enzymatically inactive MEC-17 is sufficient for the formation of the luminal material. Such a localization for MEC-17 and ATAT-2 would be consistent with the prediction by Nogales et al. [29] that Lys 40 for α-tubulin faces the MT lumen, the finding by Akella et al. [21] that αTAT acetylation occurs at the ends of axonemes, and our finding that the internal material is abundant in TRN MTs, which have MEC-17 and ATAT-2, and sparse in other neuronal MTs.

We have not determined whether MEC-17 and ATAT-2 are components of the luminal material or simply necessary for its formation. Nonetheless, the difference in the abundance of the material in WT TRN MTs compared with other neuronal MTs and the high expression of *mec-17* in the TRNs supports the contention that MEC-17 is a component of the luminal material. The need for such material and the finding that the TRN MTs elongate during larval development [10] may explain why *mec-17* mRNA is found throughout the TRN processes. Elongation may require newly synthesized MEC-17 at the site of MT growth.

MEC-17-Driven Tubulin Acetylation Helps Determine Protofilament Number

One of the most surprising aspects of our analysis is that the MTs in *mec-17* mutants fail to have the 15-p structure seen in the WT cells, despite the presence of the MEC-12 α-tubulin and the MEC-7 β-tubulin (expression is inferred from the finding that mutations in either tubulin gene suppresses much of the *mec-17* phenotype), an indication that the tubulin alone cannot determine protofilament number. This finding and the observation that the enzymatic component of MEC-17, but not ATAT-2, is required to produce 15-p MTs in the TRNs imply that MEC-17-driven acetylation of α-tubulin and/or of another substrate provides protofilament number fidelity.

Because the MTs that occur in the TRNs of *mec-17* animals usually have 13 protofilaments and not the 11 seen in non-TRN MTs in WT animals [10], MEC-17 is not the only molecule that determines protofilament number. Other candidates include MEC-12 α-tubulin and MEC-7 β-tubulin, proteins that are highly expressed in the TRNs. Support for this speculation comes from the finding that mutation of *mec-7* leads to the production of 11-p MTs in the TRNs [10].

MEC-17 Is Needed for MT Organization

Several observations suggest that loss of MEC-17 causes morphological defects (bends, swellings, branches, and extensions) in TRNs because MT structure is disrupted. These changes occur at a time when the amount of polymerized MTs increases in the WT [10] and depend on both the MEC-12 α-tubulin and the MEC-7 β-tubulin. The suppression of these phenotypes by treatment with colchicine (even in a *dlk-1* background) argues that these defects require intact MTs.

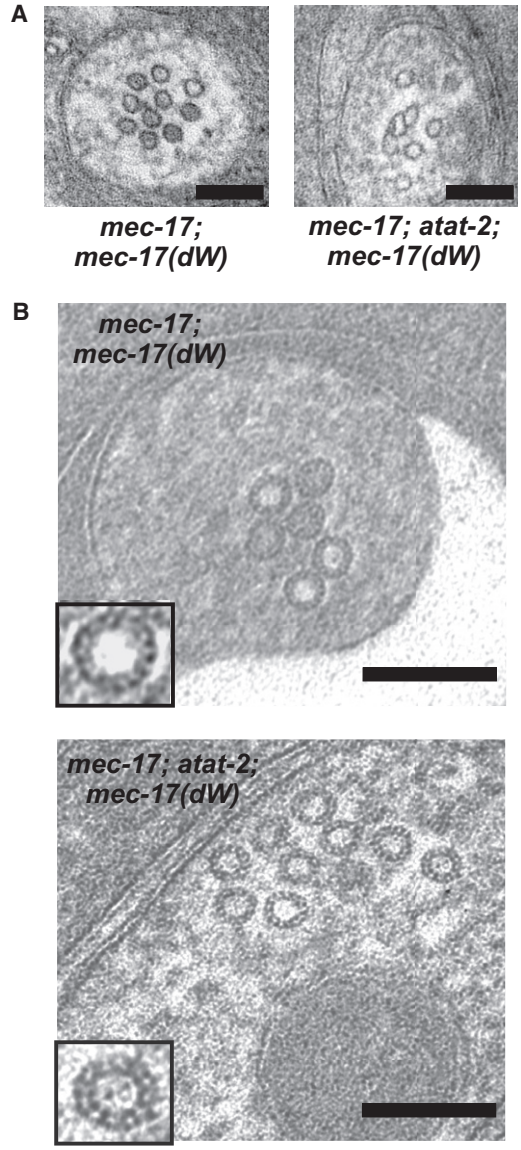

Figure 7. Enzymatically Inactive MEC-17 Does Not Rescue the MT and Protofilament Defects

(A) Electron micrographs of ALM neurons in *mec-17* and *mec-17; atat-2* mutant animals expressing the enzymatically inactive *mec-17(dW).* Scale bars throughout represent 100 nm. Left panel had HPF using 1.5% tannic acid + 0.5% glut; right panel used HPF in osmium and/or acetone (no tannic acid).

(B) Tannic acid stained *mec-17; mec-17(dW)* and *mec-17; atat-2; mec-17(dW)* mutant MTs containing 13-p, 14-p, and 15-p protofilaments. Animals were fixed in HPF using 0.25% tannic acid and 0.5% glut.

First, the decoration of the *mec-17* MT by hooks and the appearance of doublet MTs suggests that the cells produce a superabundance of the MEC-12 α-tubulin and the MEC-7 β-tubulin. When MTs are polymerized in the presence of high concentrations of tubulin dimers, sheets of protofilaments, which appear as hooks in cross-section, are often seen and have been used to determine MT orientation [38, 39]. The reduction in MT number without a reduction in the amount of tubulin dimer produced could lead to the appearance of the hooks. Although the absolute number of hooks we have seen is small, the finding that most curve in a clockwise manner is consistent with previous experiments suggestion that neuronal MTs have their plus ends distal to the cell body [38].

Second, although WT TRNs contain all their MTs in a single bundle, *mec-17* TRNs do not, indicating that the association of the MTs is disrupted in *mec-17* animals. Electron micrographs reveal that *mec-17* MTs often separate from the bundle (Figure 4; Figure S3). Moreover, the MTs in *mec-17* TRNs, which in WT remain in register with one another as they course through the neuronal process, rarely keep the same neighbors (Figure 4). A disruption of the interactions among the MTs could cause them to pack differently from the arrangement seen in wild-type cells, and this packing (perhaps aided by the increase in free tubulin dimers) could cause elongation of the process.

The 15-p MTs of WT animals form numerous cross-bridges with adjacent MTs [30, 40]. Although in the present study we had difficulty resolving MT cross-bridges in electron tomograms of either WT or mutant TRNs, we hypothesize that the change in protofilament number (and its variability) may prevent the formation (through misalignment) of some cross-bridges. Because MTs, especially in the regions of swelling, appear to bend together, not all of the interactions between MTs are missing.

Third, the changes in the structure of MTs and/or in their interaction with each other could decrease the rigidity of individual MTs or the bundle of MTs. In support of the hypothesis that formation of bundles of 15-p MTs can change the rigidity of cells, K. Szarama (personal communication) found that stiffness of pillar cells increases when acetylated 15-p MTs are made.

A loss of rigidity in the TRNs could produce several of the morphological defects seen in the *mec-17* TRNs. The TRNs processes are constantly shortening and lengthening as animals move in their usual sinusoidal fashion. If the MTs are locally flexible, the shortening could cause the MTs to buckle, producing the swellings and wavy processes. Finally, the buckling MTs, especially if some breakage occurs during the buckling, may initiate the formation of the ectopic branches, which are seen to emanate from the swellings. The many breaks in MTs seen in the tomogram of the swelling may render the *mec-17* mutant MTs more fragile.

Thus, all the morphological defects seen in the mutant TRNs could be due to changes in the MTs and their bundles. When 15-p MTs occur in other organisms ([3, 8, 9]), the MTs are also found in organized arrays that are similar to the TRN bundles. We suggest that MEC-17 and other αTATs modulate MT structure so they can form coherent MT bundles.

Conclusion

We have used the *C. elegans* TRNs, neurons that express the TRN-specific α-TAT MEC-17 and contain well-characterized 15-protofilament microtubules, to show that a tubulin acetyltransferase is needed to determine higher order structure in MTs. We show that MEC-17-driven tubulin acetylation defines protofilament number, MT number, and MT organization in the TRNs. These α-TAT-induced changes in microtubule structure affect neuronal morphology. Moreover, in addition to functioning as a α-TAT, MEC-17 acts nonenzymatically for optimal mechanosensation and TRN process extension. Our study reveals a dual function for α-TAT enzymes and proves a specific role for α-tubulin acetylation in the production of MT arrays.

Experimental Procedures

General Procedures

Unless otherwise indicated, strains were maintained and studied at 20° according to Brenner [41] on the OP50 strain of *E. coli*. The Supplemental Information contains detailed information on the strains, plasmid constructs, microinjections and microscopy, and immunofluorescence.

Colchicine Treatment

The effects of colchicine were tested by growing animals for two generations on standard nematode growth medium (NGM) agar plates [41] containing 1 mM colchicine [10].

Touch Assays

We assayed gentle touch sensitivity in blind tests as described [26]. We quantified the response by counting the number of responses to ten touches delivered alternately near the head and tail in 20 or 30 animals (or 20 or 30 characterized transformants in strains with extragenic arrays).

SM-FISH

We performed FISH as described previously [42].

Electron Microscopy

Animals were cultured for several generations on standard NGM plates and prepared for transmission electron microscopy using standard methods [43]. Adults were fixed with 3.5% glutaraldehyde and 1% paraformaldehyde in 0.12 M sodium cacodylate. Eighty-nanometer transverse sections were cut and poststained with uranium acetate and lead citrate. A Philips CM10 electron microscope with an attached Morada digital camera (Olympus) was used to acquire the images.

Tannic acid fixations were tested under multiple protocols to optimize staining. Good results came from chemical fixation in the presence of 1% tannic acid and buffered 1% gluteraldehyde for 16 hr at room temperature, buffer rinses, and fixation in osmium tetroxide, before dehydration and infiltration into Eponate resin [10]. Alternately, the first fixation was conducted by high-pressure freezing in the presence of 0.25% tannic acid and 0.5% gluteraldeyde in acetone, followed by freeze substitution over 5 days and a subsequent osmium in acetone fixation, prior to plastic embedment.

For electron tomography, animals were fixed by high-pressure freezing and freeze substitution using standard methods and embedded into plastic [43]. Semithin serial sections (100–250 nm thick) were collected and viewed on an FEI Technai20 electron microscope. Each section was viewed at high resolution under multiple tilts to produce two single axis tomograms using markerless alignment procedures and internal features to create weighted backprojection models of the tissue in 3D space [43, 44]. Two single axis tilt tomograms were then combined to create a dual axis tomogram having higher resolution, and tomograms from several serial sections were then melded to produce a larger electron tomogram that spanned about 1 μm in the z dimension. The IMOD software package [45] was used to annotate each tomogram by hand.

Supplemental Information

Supplemental Information includes four figures, Supplemental Experimental Procedures, and one movie and can be found with this article online at doi:10.1016/j.cub.2012.03.066.

Acknowledgments

We thank Katherine Szarama for comments on the manuscript and permission to cite her unpublished data. We acknowledge the help and advice of Bill Rice and K.D. Derr (NY Structural Biology Center) for their help and encouragement in performing electron tomography procedures and Leslie Gunther and Juan Jimenez (Analytical Imaging Facility, Einstein) for their help in conducting high-pressure freezing. Ken McDonald kindly provided tannic acid samples for our fixations. Some nematode strains used in this work were provided by the Caenorhabditis Genetic Center, which is funded by the National Institutes of Health (NIH) National Center for Research Resources. Use of electron tomography facilities at NYSBC was supported by the Albert Einstein College of Medicine. N.K. was supported by an EMBO Short Term Fellowship (ASTF 362-1010). This work was supported by grants GM30997 to M.C. and OD010943 to D.H.H. from the NIH.

Received: February 6, 2012
Revised: March 19, 2012
Accepted: March 19, 2012
Published online: May 31, 2012

References

1. Tilney, L.G., Bryan, J., Bush, D.J., Fujiwara, K., Mooseker, M.S., Murphy, D.B., and Snyder, D.H. (1973). Microtubules: evidence for 13 protofilaments. J. Cell Biol. *59*, 267–275.
2. Burton, P.R., and Hinkley, R.E. (1974). Further electron miscroscopic characterization of axoplasmic microtubules of the ventral cord of the crayfish. J. Submicrosc. Cytol. *6*, 311–326.
3. Burton, P.R., Hinkley, R.E., and Pierson, G.B. (1975). Tannic acid-stained microtubules with 12, 13, and 15 protofilaments. J. Cell Biol. *65*, 227–233.
4. Afzelius, B.A., Bellon, P.L., and Lanzavecchia, S. (1990). Microtubules and their protofilaments in the flagellum of an insect spermatozoon. J. Cell Sci. *95*, 207–217.
5. Hirose, K., Amos, W.B., Lockhart, A., Cross, R.A., and Amos, L.A. (1997). Three-dimensional cryoelectron microscopy of 16-protofilament microtubules: structure, polarity, and interaction with motor proteins. J. Struct. Biol. *118*, 140–148.
6. Raff, E.C., Fackenthal, J.D., Hutchens, J.A., Hoyle, H.D., and Turner, F.R. (1997). Microtubule architecture specified by a beta-tubulin isoform. Science *275*, 70–73.
7. Eichenlaub-Ritter, U., and Tucker, J.B. (1984). Microtubules with more than 13 protofilaments in the dividing nuclei of ciliates. Nature *307*, 60–62.
8. Nagano, T., and Suzuki, F. (1975). Microtubules with 15 subunits in cockroach epidermal cells. J. Cell Biol. *64*, 242–245.
9. Saito, K., and Hama, K. (1982). Structural diversity of microtubules in the supporting cells of the sensory epithelium of guinea pig organ of Corti. J. Electron Microsc. (Tokyo) *31*, 278–281.
10. Chalfie, M., and Thomson, J.N. (1982). Structural and functional diversity in the neuronal microtubules of *Caenorhabditis elegans*. J. Cell Biol. *93*, 15–23.
11. Davis, C., and Gull, K. (1983). Protofilament number in microtubules in cells of two parasitic nematodes. J. Parasitol. *69*, 1094–1099.
12. Binder, L.I., and Rosenbaum, J.L. (1978). The in vitro assembly of flagellar outer doublet tubulin. J. Cell Biol. *79*, 500–515.
13. Pierson, G.B., Burton, P.R., and Himes, R.H. (1978). Alterations in number of protofilaments in microtubules assembled in vitro. J. Cell Biol. *76*, 223–228.
14. McEwen, B., and Edelstein, S.J. (1980). Evidence for a mixed lattice in microtubules reassembled in vitro. J. Mol. Biol. *139*, 123–145.
15. Linck, R.W., and Langevin, G.L. (1981). Reassembly of flagellar B (alpha beta) tubulin into singlet microtubules: consequences for cytoplasmic microtubule structure and assembly. J. Cell Biol. *89*, 323–337.
16. Scheele, R.B., Bergen, L.G., and Borisy, G.G. (1982). Control of the structural fidelity of microtubules by initiation sites. J. Mol. Biol. *154*, 485–500.
17. Aamodt, E.J., and Culotti, J.G. (1986). Microtubules and microtubule-associated proteins from the nematode *Caenorhabditis elegans*: periodic cross-links connect microtubules in vitro. J. Cell Biol. *103*, 23–31.
18. Meurer-Grob, P., Kasparian, J., and Wade, R.H. (2001). Microtubule structure at improved resolution. Biochemistry *40*, 8000–8008.
19. Moores, C.A., Perderiset, M., Francis, F., Chelly, J., Houdusse, A., and Milligan, R.A. (2004). Mechanism of microtubule stabilization by doublecortin. Mol. Cell *14*, 833–839.
20. Chalfie, M., and Au, M. (1989). Genetic control of differentiation of the *Caenorhabditis elegans* touch receptor neurons. Science *243*, 1027–1033.
21. Akella, J.S., Wloga, D., Kim, J., Starostina, N.G., Lyons-Abbott, S., Morrissette, N.S., Dougan, S.T., Kipreos, E.T., and Gaertig, J. (2010). MEC-17 is an alpha-tubulin acetyltransferase. Nature *467*, 218–222.
22. Shida, T., Cueva, J.G., Xu, Z., Goodman, M.B., and Nachury, M.V. (2010). The major alpha-tubulin K40 acetyltransferase alphaTAT1 promotes rapid ciliogenesis and efficient mechanosensation. Proc. Natl. Acad. Sci. USA *107*, 21517–21522.
23. LeDizet, M., and Piperno, G. (1987). Identification of an acetylation site of Chlamydomonas alpha-tubulin. Proc. Natl. Acad. Sci. USA *84*, 5720–5724.

24. Zhang, Y., Ma, C., Delohery, T., Nasipak, B., Foat, B.C., Bounoutas, A., Bussemaker, H.J., Kim, S.K., and Chalfie, M. (2002). Identification of genes expressed in *C. elegans* touch receptor neurons. Nature *418*, 331–335.
25. Topalidou, I., and Chalfie, M. (2011). Shared gene expression in distinct neurons expressing common selector genes. Proc. Natl. Acad. Sci. USA *108*, 19258–19263.
26. Chalfie, M., and Sulston, J. (1981). Developmental genetics of the mechanosensory neurons of *Caenorhabditis elegans*. Dev. Biol. *82*, 358–370.
27. Savage, C., Hamelin, M., Culotti, J.G., Coulson, A., Albertson, D.G., and Chalfie, M. (1989). mec-7 is a beta-tubulin gene required for the production of 15-protofilament microtubules in *Caenorhabditis elegans*. Genes Dev. *3*, 870–881.
28. Fukushige, T., Siddiqui, Z.K., Chou, M., Culotti, J.G., Gogonea, C.B., Siddiqui, S.S., and Hamelin, M. (1999). MEC-12, an alpha-tubulin required for touch sensitivity in *C. elegans*. J. Cell Sci. *112*, 395–403.
29. Nogales, E., Whittaker, M., Milligan, R.A., and Downing, K.H. (1999). High-resolution model of the microtubule. Cell *96*, 79–88.
30. Chalfie, M., and Thomson, J.N. (1979). Organization of neuronal microtubules in the nematode *Caenorhabditis elegans*. J. Cell Biol. *82*, 278–289.
31. Moerman, D.G., and Barstead, R.J. (2008). Towards a mutation in every gene in *Caenorhabditis elegans*. Brief. Funct. Genomics Proteomics *7*, 195–204.
32. Piperno, G., and Fuller, M.T. (1985). Monoclonal antibodies specific for an acetylated form of alpha-tubulin recognize the antigen in cilia and flagella from a variety of organisms. J. Cell Biol. *101*, 2085–2094.
33. Bounoutas, A., Kratz, J., Emtage, L., Ma, C., Nguyen, K.C., and Chalfie, M. (2011). Microtubule depolymerization in *Caenorhabditis elegans* touch receptor neurons reduces gene expression through a p38 MAPK pathway. Proc. Natl. Acad. Sci. USA *108*, 3982–3987.
34. Steczkiewicz, K., Kinch, L., Grishin, N.V., Rychlewski, L., and Ginalski, K. (2006). Eukaryotic domain of unknown function DUF738 belongs to Gcn5-related N-acetyltransferase superfamily. Cell Cycle *5*, 2927–2930.
35. Pulak, R., and Anderson, P. (1993). mRNA surveillance by the *Caenorhabditis elegans smg* genes. Genes Dev. *7*, 1885–1897.
36. Zilberman, Y., Ballestrem, C., Carramusa, L., Mazitschek, R., Khochbin, S., and Bershadsky, A. (2009). Regulation of microtubule dynamics by inhibition of the tubulin deacetylase HDAC6. J. Cell Sci. *122*, 3531–3541.
37. Garvalov, B.K., Zuber, B., Bouchet-Marquis, C., Kudryashev, M., Gruska, M., Beck, M., Leis, A., Frischknecht, F., Bradke, F., Baumeister, W., et al. (2006). Luminal particles within cellular microtubules. J. Cell Biol. *174*, 759–765.
38. Heidemann, S.R., and McIntosh, J.R. (1980). Visualization of the structural polarity of microtubules. Nature *286*, 517–519.
39. McIntosh, J.R., and Euteneuer, U. (1984). Tubulin hooks as probes for microtubule polarity: an analysis of the method and an evaluation of data on microtubule polarity in the mitotic spindle. J. Cell Biol. *98*, 525–533.
40. Cueva, J.G., Mulholland, A., and Goodman, M.B. (2007). Nanoscale organization of the MEC-4 DEG/ENaC sensory mechanotransduction channel in *Caenorhabditis elegans* touch receptor neurons. J. Neurosci. *27*, 14089–14098.
41. Brenner, S. (1974). The genetics of *Caenorhabditis elegans*. Genetics *77*, 71–94.
42. Topalidou, I., van Oudenaarden, A., and Chalfie, M. (2011). *Caenorhabditis elegans aristaless/Arx* gene *alr-1* restricts variable gene expression. Proc. Natl. Acad. Sci. USA *108*, 4063–4068.
43. Hall, D.H., Hartwieg, E., and Nguyen, K.C. (2012). Modern electron microscopy methods for *C. elegans*. Methods Cell Biol. *107*, 93–149.
44. Franck, J. (2006). Electron Tomography: Methods for the three-dimensional visualization of structure in the cell, Second Edition (New York: Springer), pp. 455.
45. Kremer, J.R., Mastronarde, D.N., and McIntosh, J.R. (1996). Computer visualization of three-dimensional image data using IMOD. J. Struct. Biol. *116*, 71–76.